AIAA JOURNAL
Vol. 42, No. 5, May 2004

Effect of Spanwise-Modulated Disturbances on Transition in a Separated Boundary Layer

Olaf Marxen,* Ulrich Rist,† and Siegfried Wagner‡
University of Stuttgart, D-70550 Stuttgart, Germany

A laminar boundary layer separates in a region of adverse pressure gradient on a flat plate and undergoes transition. The detached shear layer rolls up into spanwise vortices that rapidly break down into small-scale turbulence. Finally, the turbulent boundary layer reattaches, forming a laminar separation bubble. Development and role of three-dimensional disturbances for transition in such a separation bubble are studied by means of direct numerical simulation with controlled disturbance input. In the present case, the level of incoming three-dimensional perturbations is not relevant due to an absolute secondary instability of these disturbances in the region of convective two-dimensional shear layer rollup. In particular, this is true for steady perturbations up to moderate amplitudes. Following their generation by nonlinear interaction of disturbance waves in the region of favorable pressure gradient, these steady disturbances develop as streaks. Their downstream evolution can be first attributed to transient behavior, depending on initial excitation, followed by a universal state with characteristics of a modal instability. Numerical results are confirmed by a comparison with experimental data.

Nomenclature

A	=	flow cases including the whole laminar separation bubble (LSB)
B	=	flow cases including only the first part of the LSB
f	=	frequency, 1/s
j	=	index of a grid point in wall-normal direction
k, h	=	harmonic(s) in Fourier space, real wave number coefficient in spanwise direction and in time
n	=	grid point(s) in physical space
P	=	Gaster's[22] pressure gradient parameter
Re_s	=	Reynolds number based on length s
u, v, w	=	velocities, m/s
x, y, z	=	Cartesian axes, m
β	=	Falkner–Skan parameter
δ_1	=	displacement thickness, m
δ_2	=	momentum thickness, m
κ	=	grid-stretching parameter
λ	=	wavelength, m
ν	=	kinematic viscosity, m^2/s

Subscripts

L	=	length of integration domain
max	=	maximum in wall-normal direction
R	=	mean reattachment position
ref	=	reference quantity, used for nondimensionalization
S	=	mean separation position
x	=	streamwise direction
y	=	wall-normal direction
z	=	spanwise direction
0	=	fundamental frequency
02	=	small-amplitude disturbance (0, 2)
∞	=	freestream for the plate without pressure gradient

Superscripts

02	=	large-amplitude disturbance (0, 2)
$'$	=	disturbance quantity
$\hat{}$	=	amplitude

Introduction

TRANSITION to turbulence in a two-dimensional separated boundary layer often leads to reattachment of the turbulent boundary layer and the formation of a laminar separation bubble (LSB). In environments with a low level of disturbances fluctuating in time, the transition process is governed by strong amplification of these disturbances. Such a scenario is typical for a pressure-induced LSB, for example, found on a (glider) wing in free flight, or for an experiment where the region of pressure rise is preceded by a favorable pressure gradient that damps out unsteady perturbations.[1] In the region of an adverse pressure gradient, disturbances are subject to strong amplification, and their saturation leads to shear layer rollup and vortex shedding. This vortex shedding is often essentially a two-dimensional phenomenon, that is, strong spanwise coherence of the vortex structure, caused by either spanwise constant (two-dimensional) small-amplitude waves or by spanwise-harmonic (three-dimensional) waves with small obliqueness angles in an otherwise undisturbed flow. According to a classification by Rist and Maucher,[2] amplification of these waves can proceed via a gradual switchover from a viscous wall-mode instability [so called Tollmien–Schlichting (TS) instability] toward an inviscid free shear-layer type instability (Kelvin–Helmholtz instability), distinguishable by the position and strength of the maximum in the disturbance-amplitude function.

Considerable discussion is still going on as to the origin and role of disturbances with strong spanwise variation in an LSB. Two distinct forms of three-dimensional disturbances are commonly observed: steady and highly fluctuating. In the past, presence of steady perturbations in separated flows was commonly attributed to Görtler vortices (see Refs. 3–5). Amplification of such streamwise vortices is caused by the effect of streamline curvature. Research of bypass transition in zero pressure-gradient boundary layers revealed the possibility of transient growth of steady spanwise disturbances that are often referred to as streaks.[6] Presence of streaks in conjunction with separated flows was experimentally observed by Watmuff.[1] The development of such streaks in separated boundary layers and their relation to transient growth has only recently been studied experimentally and theoretically.[7]

Growth of perturbations fluctuating in time is occasionally attributed to a (classical) secondary instability known from K-type

Presented as Paper 2003-0789 at the 41st Aerospace Sciences Meeting, Reno, NV, 6–9 January 2003; received 11 March 2003; revision received 4 December 2003; accepted for publication 18 January 2004.

*Research Assistant, Institut für Aerodynamik und Gasdynamik.
†Senior Research Scientist, Institut für Aerodynamik und Gasdynamik.
‡Professor, Institut für Aerodynamik und Gasdynamik. Member AIAA.

boundary-layer transition with its peak–valley splitting.[8] However, it was concluded by Rist[9] that such a scenario, analyzable by Floquet theory, contributes only marginally to transition in LSBs. Instead, breakdown of weakly oblique traveling waves as the probably fastest route to turbulence is proposed; still, breakdown scenarios depend considerably on LSB size and local Reynolds number of the separated boundary layer. A mechanism of absolute secondary instability of three-dimensional disturbances in separation bubbles was discovered by Maucher et al.[10] for fairly strong pressure gradients and/or high local Reynolds number $Re_{\delta_1}^{x=x_s}$ based on the displacement thickness δ_1 at separation. It appears to the authors that in Ref. 11 a somewhat similar mechanism of absolute secondary instability was observable, which lead to sudden transition with immediate occurrence of three dimensionality, although it was not recognized as such there. Instead, it was stated there that the flowfield is not analyzable in terms of primary or secondary instability.

The present study shall provide an insight into possible instability mechanisms leading to amplification of spanwise-harmonic disturbances in an LSB and their importance for the transition process. It is divided into two parts, the first concerned with fluctuating disturbances and the second part with steady perturbations. The subject is studied by means of direct numerical simulations (DNS) with controlled disturbance input, designed to model closely an experiment carried out at the Institut für Aerodynamik und Gasdynamik, which serves as a reference case.

Description of the Flow

The reference case is defined by an experimental setup specified in detail in Refs. 12–14. Only a brief description shall be given here. A flat plate was mounted in the freestream ($U_\infty = 0.125$ m/s $\approx 0.75 U_{\text{ref}}$, which results in a Reynolds number per meter of $\approx 1.7 \times 10^5$ m^{-1}) of the test section of a laminar water tunnel. A streamwise pressure gradient was imposed locally on the flat-plate boundary layer by a displacement body, inducing a region of favorable pressure gradient followed by a pressure rise (Figs. 1a and 1b). In the region of adverse pressure gradient (starting at $x \approx 0$ mm), a laminar separation bubble developed (Fig. 1c) between the points of separation, S and mean reattachment, R. The transition experiment was performed with controlled disturbance input. A two-dimensional time-harmonic perturbation was introduced upstream of the displacement body ($x = -230$ mm) by an oscillating wire (fundamental frequency $f_0 = 1.1$ Hz). Additionally, three-dimensional disturbances were imposed by placing thin (1.0-mm) metal plates (spacers) regularly underneath the wire (fundamental spanwise wavelength $\lambda_z = 58$ mm). Phase-averaged and

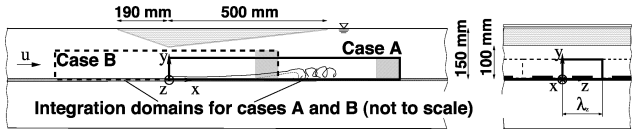

a) Experimental setup and numerical integration domains

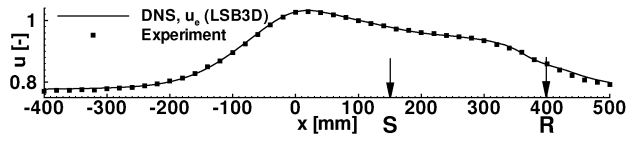

b) Streamwise velocity at a constant distance from the wall, $y = 50$ mm

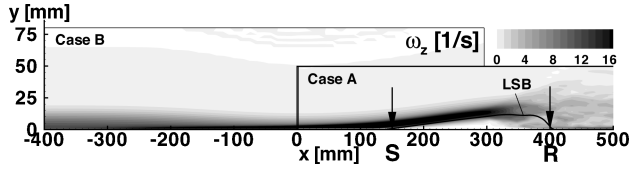

c) Contours of spanwise vorticity $\omega_z = \partial u/\partial y - \partial v/\partial x$ from DNS (LSB3D) together with dividing streamline

Fig. 1 Experimental and numerical setup and time- and spanwise-averaged flow quantities.

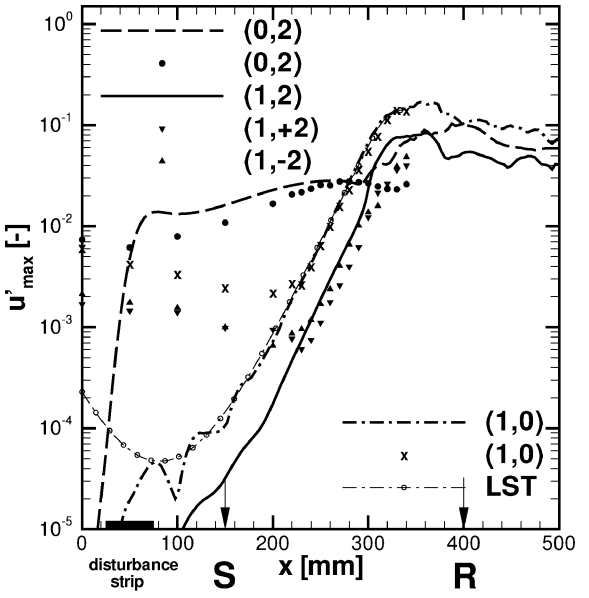

Fig. 2 Amplification of the maximum two- and three-dimensional streamwise velocity fluctuation u'_{max}; lines, DNS; symbols, LDA; and LST (case LSB3D, taken from Ref. 14).

phase-locked data acquisition[12] allowed for spectral decomposition in time and spanwise direction of measured data.

For the calculations, general physical parameters of the flow are chosen to match this setup as close as possible. At a streamwise position $x = -400$ mm, the observed boundary-layer profile can be approximated by a Falkner–Skan similarity solution ($Re_{\delta_1} = 900$, $\beta = 1.03$) and is used as inflow condition. In contrast to the experiment, in the numerical simulations different combinations of the disturbance input are chosen. Velocities are nondimensionalized using a pseudo-potential velocity at the wall in the narrowest cross section at $x = 0$ mm. The procedure to obtain this velocity U_{ref} is described by Marxen et al.[14]

In previous works,[12,14] it was shown that numerical results and measurements obtained by laser Doppler anemometry as well as predictions from linear stability theory (LST) agree very well for time-averaged (Fig. 1b) and two-dimensional time-harmonic quantities (Fig. 2). In this study, further insight into the impact of spanwise-modulated disturbances of small to medium amplitude on the transition process will be gathered. Results from Ref. 14 serve as a reference, and physical processes occurring in this reference case will be briefly described as follows.

The first section of the LSB is dominated by a primary convective instability of a two-dimensional TS wave of fundamental frequency. Figure 2 (taken from Marxen et al.[14]) shows that the TS wave (1, 0) is strongly amplified in the region of adverse pressure gradient. Good agreement of both experimental and numerical results with LST from $x = 230$ mm onward confirms the primary convective nature of this disturbance. Furthermore, with a maximum observable reverse flow velocity below 10% of the freestream velocity, the occurence of an absolute primary instability is very unlikely according to Alam and Sandham[15] and Rist and Maucher.[2] Saturation of the TS wave leads to shear layer rollup followed by vortex shedding with the fundamental frequency. Breakdown into small-scale three-dimensional turbulence occurs around the position of saturation of the fundamental wave. In Ref. 14 it was stated that oblique waves eventually cause breakdown into turbulence. These waves emerge from nonlinear interaction of a large steady three-dimensional and the fundamental two-dimensional disturbance as was found by additional calculations.

The present study serves to prove the preceding described picture of the transition process in the LSB by discussing the results of these additional calculations and their implications. In addition, conclusions drawn from these calculations justify the application of a calculation method normally not applicable for separated flows.

This method is based on a disturbance formulation and is well suited to clarify the origin of steady disturbances and their impact on the transition process in LSBs. Because time-harmonic disturbances nonlinearly generate steady ones, it is not meaningful here to exclude one or the other of these disturbances from the calculations by, for example, solving time-averaged equations.

Numerical Method

Spatial DNS of the three-dimensional incompressible Navier–Stokes equations serves to compute the accelerated and decelerated boundary layer described in the preceding section. Two different methods are applied for the examination of fluctuating (case A) and steady (case B) three-dimensional disturbances. Both methods use finite differences on a Cartesian grid for downstream and wall-normal discretization, whereas a spectral ansatz is applied in spanwise direction. An explicit fourth-order Runge–Kutta scheme is used for time integration. Upstream of the outflow boundary, a buffer domain smoothly returns the flow to a steady laminar state. An additional damping zone at the upper boundary prevents reflections of disturbances in the turbulent part of the boundary layer. Disturbances of arbitrary frequency can be introduced via blowing and suction at the wall through a disturbance strip. To reduce computational effort, spanwise symmetry is assumed for calculations.

Cases A make use of fourth-order accurate finite differences on an equidistant grid. Because this method is applied when the integration domain contains the whole separation bubble, inviscid–viscous interaction due to boundary-layer displacement must be accounted for. The displacement depends on the size of the LSB, which is not known a priori, but instead is a result of the calculation. Numerical method A is described in detail in Refs. 14 and 16.

The method for cases B is of sixth-order accuracy and allows for grid stretching in the wall-normal direction. For integration domains that contain only the first part of the LSB, it is meaningful to distinguish between a two-dimensional steady base flow and unsteady perturbations, so that a disturbance formulation is applicable. This will be further explained in a later section. Numerical method B is described in detail in Ref. 17. In comparison to Ref. 17, the calculation of coefficients for finite differences is altered to allow for nonequidistant grids in wall-normal direction.

A double Fourier transform in time and spanwise direction of data sets from measurements or simulations yields disturbance amplitudes and phases. The notation (h, k) will be used to specify the modes, with h and k denoting wave-number coefficients in the time and spanwise direction, respectively.

For simulations of case A, the separation bubble showed low-frequency oscillations (so-called flapping) so that the Fourier analysis had to be carried out using a Hanning-window function to suppress aliasing effects. Four periods of the fundamental frequency were used in the analysis. The subharmonic was checked to have low-amplitude and taken as proof that frequencies of the flapping and of the vortex shedding were indeed well separated.

Time-Harmonic Three-Dimensional Disturbances

Because turbulence is characterized by highly fluctuating three-dimensional disturbances, in this section the role of unsteady spanwise-harmonic disturbances for the transition process will be clarified. This is achieved by variation of the number, type, and amplitude of the three-dimensional disturbance input.

Despite the importance of three-dimensional perturbations for the breakdown process, transition is dominated by the convectively unstable two-dimensional TS wave.[14] A two-dimensional disturbance input has a strong impact on the size of the LSB and is necessary for good agreement with experimental results, as shown, for example, by Maucher et al.[16] However, the role of this type of disturbance appears clear, as was also shown by Rist et al.[18] that the initial amplitude of the fundamental two-dimensional wave is responsible for the overall size of a forced LSB. Therefore, no variation of its amplitude is presented here.

Table 1 Disturbance v-amplitudes for cases A

Case	(1, 0)	(0, 2)	(1, 2)
LSB3D	7×10^{-6}	1.82×10^{-3}	——
A_{02}	9×10^{-6}	4×10^{-4}	——
A^{02}	9×10^{-6}	6.8×10^{-4}	——
A^{02}_{12}	9×10^{-6}	6.8×10^{-4}	2×10^{-5}
A_{02-12}	9×10^{-6}	1.8×10^{-4}	2×10^{-5}
A_{no3D}	9×10^{-6}	——	——

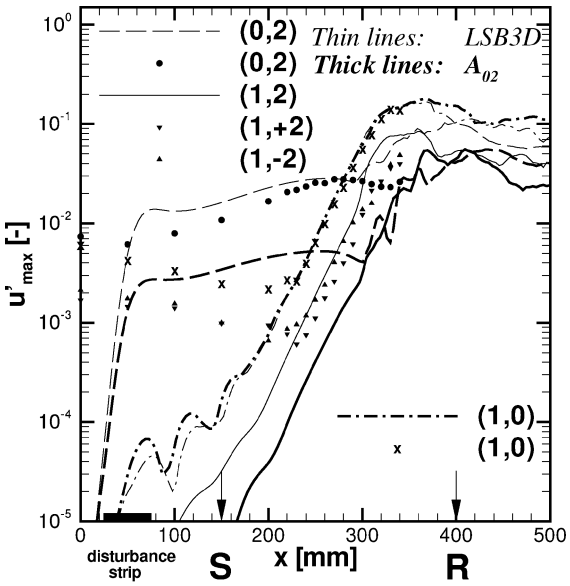

Fig. 3 Same as Fig. 2; comparison of reference case LSB3D with case A_{02}.

Test Cases A

In all cases A, a small-amplitude two-dimensional time-harmonic wave (1, 0) with the same amplitude is forced upstream of the LSB. Additional steady and/or time-harmonic, as well as spanwise-harmonic, disturbances are excited with varying amplitudes. Disturbance amplitudes for the wall-normal velocity for several calculations are given in Table 1. The notation used indicates whether disturbance amplitude is high (superscript) or low (subscript).

The integration domain (Fig. 1a) starts at $x = 0$ mm. Its streamwise and wall-normal extent was $x_L = 812$ mm and $y_L = 50$ mm, respectively. The spanwise extent is a single-spacer wavelength λ_z. The number of grid points n and modes k is $n_x \times n_y \times k_z = 1778 \times 185 \times 27$. The discretization in x results in approximately 120 grid points per streamwise wavelength of the fundamental wave. The last 246 grid points in x and the topmost 20 grid points in y are used as buffer zones, where the flow is gradually ramped to a laminar state. Resolution in time is 600 time steps per fundamental period. The disturbance strip is 120 grid points in length and centered at $n_x = 120$.

Before discussing the results, let us briefly illustrate the concept of nonlinear disturbance generation. As a result of the nonlinear terms in the Navier–Stokes equations, two disturbances of the streamwise velocity $u_1 = \hat{U}_1 \cdot \exp(ih_1 \cdot t + ik_1 \cdot z)$ and $u_2 = \hat{U}_2 \cdot \exp(\pm ih_2 \cdot t \mp ik_2 \cdot z)$ cause a disturbance $u_1 \cdot u_2 \approx \hat{U}_1 \hat{U}_2 \cdot \exp[i(h_1 \pm h_2) \cdot t + i(k_1 \mp k_2) \cdot z]$, for example, mode (1, 0) and mode (0, 2) will result in mode (1, 2) with an amplitude given roughly by the product of amplitudes of the generating modes. This example indicates that steady three-dimensional disturbances can play a role in generation of certain types of three-dimensional unsteady perturbations and vice versa.

Results

A comparison of reference case LSB3D vs a simulation with lower amplitude of the steady disturbance (0, 2) case A_{02} is shown in Fig. 3. Although mode (0, 2) reaches high u amplitudes (>3%

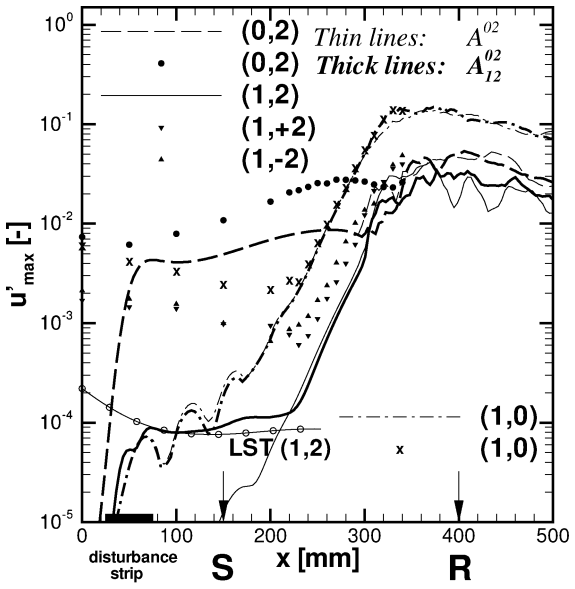

Fig. 4 Same as Fig. 2; comparison of cases A^{02} and A^{02}_{12}.

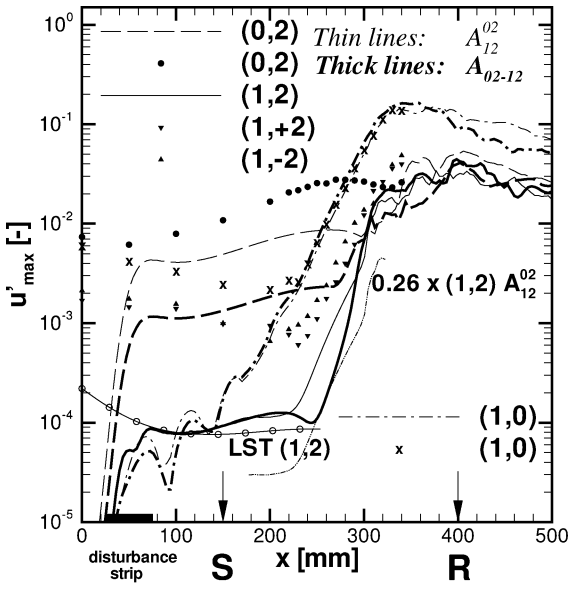

Fig. 5 Same as Fig. 2; comparison of cases A^{02}_{12} and A_{02-12}.

with respect to the local freestream velocity) in the reference case, the transition mechanism remains basically the same. In both cases, mode (1, 0) possesses the same amplitude, amplification rate, and saturation level. The three-dimensional modes (0, 2) and (1, 2) in case A_{02} show the same amplification and a comparable final saturation level as in the reference case, although they are shifted to a lower amplitude in the laminar part of the LSB ($x < 300$ mm).

As a consequence, amplification of mode (1, 2) cannot be attributed to secondary instability caused by three-dimensional distortion of the mean flow through the large steady disturbance because the growth rate would necessarily depend on the strength of the distortion of the mean flow and, thus, on the amplitude of the steady disturbance. Instead, no change in amplification rate is observed: amplitude curves of disturbances (1, 2) are parallel in Fig. 3.

To exclude a dependency on the initial amplitude of mode (1, 2), which is different in both earlier cases, an additional disturbance (1, 2) is introduced (case A^{02}_{12} vs case A^{02}, both with a slightly different amplitude of the steady disturbance compared to A_{02}). It can be seen in Fig. 4 that, from the streamwise position $x = 220$ mm onward, equal development of mode (1, 2) is observable, excluding a dependency from initial amplitude of mode (1, 2). Furthermore, the onset of strong growth of mode (1, 2) cannot be explained by linear theory, which predicts damping downstream of $x = 220$ mm (Fig. 4). The region of primary instability for this perturbation is confined to a region close to the separation point.

The reason for the deviation of amplification of mode (1, 2) from predictions of LST upstream of $x = 220$ mm (Fig. 4) is not known. Nonparallelity of the base flow might play a strong role for highly oblique waves (and the obliqueness angle of this wave ≈ 60 deg), which is neglected in the LST approach used here.[14] Despite the deviation toward higher amplification rates, growth still remains fairly small when compared to the growth due to nonlinear interaction.

If the amplitude of the steady disturbance mode (0, 2) is considerably reduced (case A_{02-12}), strong growth of mode (1, 2) is delayed farther downstream (Fig. 5). However, because amplification is slightly stronger now, the saturation level and position for mode (1, 2) show no significant difference to the earlier case A^{02}_{12}. Parallel amplitude development is confined to a small streamwise region, as illustrated by a multiplication of amplitude curve (1, 2) for case A^{02}_{12} by a factor $1.8/6.8 \approx 0.26$.

Strong amplification of mode (1, 2) in case A_{02-12} is observable from the streamwise position onward, where the TS wave has already gained high amplitude (>1%) and, thus, in later stages of the transition process. This strong amplification is confined to an even smaller streamwise region than before, and therefore, transition would appear to be sudden when amplitudes are not plotted in a logarithmic scale. This strongly resembles the secondary instability mechanism proposed by Maucher et al.[10]

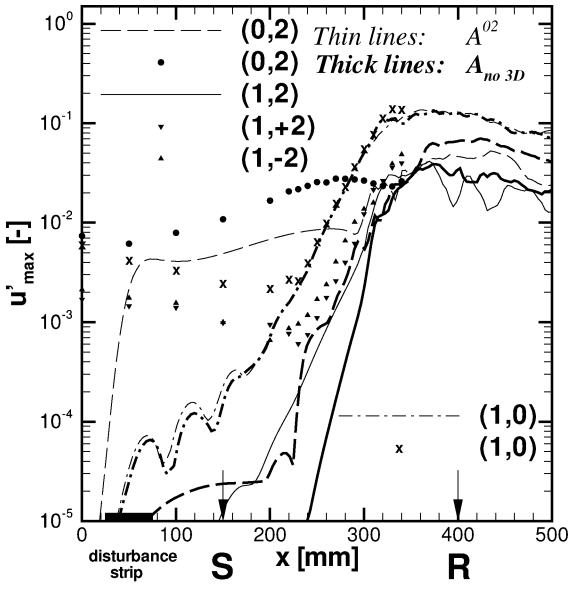

Fig. 6 Same as Fig. 2; comparison of cases A^{02} and A_{no3D}.

When switching off all three-dimensional disturbances (case A_{no3D}), it turns out that indeed such a mechanism of absolute instability with respect to three-dimensional perturbations is at work, because three-dimensional disturbances are not convected downstream and the development of modes (1, 0) and (1, 2) remains essentially the same (Fig. 6). This gives the final proof that transition in the reference case is in fact a result of an absolute secondary instability of three-dimensional disturbances in the presence of a large-amplitude TS wave as stated in Ref. 14.

Discussion

A strong spanwise modulation of the flowfield in the first part of the LSB does not exert an important influence on two-dimensional primary instability characteristics, as can be seen from the good agreement of the development of the fundamental TS wave (1, 0) with LST in all cases. This is not surprising because the most likely influence would be through a mean flow deformation caused by mode (0, 2), which should be of the order $\leq (3 \times 10^{-2})^2 \approx 10^{-3}$,

which is at least two orders of magnitude below the base flow velocity at the y position of the maximum of mode (1, 0). This observation is in line with results from Mendonça et al.,[19] who showed a suppression of amplification of TS waves only for steady spanwise perturbations with amplitudes above 10%.

Secondary instability with respect to the steady spanwise perturbation is not observable in any case with disturbance amplitudes for the streamwise velocity up to 3%. This is consistent with observations of secondary instability of Görtler vortices (see Ref. 20) with a necessary amplitude >10% or for boundary-layer streaks, where an even higher amplitude (>20%) seems necessary.[21]

The present case with a Reynolds number based on the momentum thickness δ_2 at separation $Re_{\delta_2}^{x=x_s} = 305$ and a deceleration parameter $P = {\delta_2}^2/\nu \cdot \Delta u/\Delta x \approx -0.23$ is comparable to Gaster's[22] case IV, series I. Therefore, it can be put in between the studies by Wilson and Pauley[5] with $Re_{\delta_2} = 430$ and $P = -0.28$ and Spalart and Strelets[11] with $Re_{\delta_2} = 180$ and $P = -0.1$.

A transition scenario was given in the reference case LSB3D in which a moderately growing large steady spanwise-harmonic perturbation together with a strongly amplified two-dimensional TS wave cause breakdown into turbulence by mere nonlinear interaction, as stated in the description of the flow. Such a scenario would lead to transition without involving further, that is, secondary, instabilities. However, switching off the three-dimensional disturbance input revealed that in fact a transition mechanism comparable to the one described by Maucher et al.[10] is in operation. Furthermore, there is indication that it might be the same mechanism as in Ref. 11 because there, as well as in the present case, shear layer-type instability (Kelvin–Helmholtz) is involved together with rapid onset of three dimensionality. The only difference concerns the origin of two-dimensional disturbance waves, which are explicitly forced in the present case, whereas forcing is absent in the study of Spalart and Strelets.[11] It is argued there that a receptivity mechanism might be present, acting to transform pressure fluctuations into streamwise waves. However, there also might have been reflections at or leakage through the inflow (note the streamwise periodicity) so that the disturbance level does not fall below values that are of the same order as the two-dimensional disturbance input here. (See Fig. 6 in Ref. 11.) Time-growing disturbances in conjunction with vortex shedding (which is also present here as a result of saturation of TS waves) were also observed by Pauley,[4] but were attributed to startup transients and not related to an absolute instability.

Note that, despite the presence of a large steady mode (0, 2), it is the traveling oblique wave (1, 2) that serves to break up the spanwise vortex rapidly into small-scale structures. The presence of a large steady disturbance helps to explain the growth rate of mode (1, 2) observed experimentally and to show that experimental conditions can be reproduced accurately by DNS; however, it does not play an essential role in the transition process of this LSB.

Development of Steady Three-Dimensional Disturbances

For calculations considered in this section, results from (any of the) earlier described calculations (however, with different discretization and domain size as it will be seen in the next section) were time averaged and used as a steady base flow for subsequent numerical simulations. Conclusions drawn in the last section justify such a procedure up to a streamwise position close to the transition location, ($x = 320$ mm). Change in discretization and domain size was done for verification purposes.

In the last section, it was found that even large steady three-dimensional disturbances do not change the stability behavior of the flowfield. This stability behavior is known to be very sensitive with respect to small changes of the shape of, for example the u-velocity profile. Thus, mean properties were not affected and allowed to run a case without three-dimensional disturbance input (A_{no3D}).

As can be seen from Fig. 6, up to a streamwise position of $x = 200$ mm disturbances remain below 10^{-3}, so that their possible contribution to the base flow due to nonlinear interaction should be of the order of 10^{-6}. A solution to the full three-dimensional Navier–Stokes equations that is converged to a steady two-dimensional state with an error of $\mathcal{O}(10^{-6})$ can be regarded as a steady two-dimensional solution of the Navier–Stokes equations and is, therefore, usable as a base flow in subsequent disturbance calculations. The useful region of such a calculation reaches up to $x \approx 220$ mm, then is followed by a buffer domain of one fundamental wavelength, which ends at the outflow.

Note that the time-averaged flowfield in the first part of the LSB can only be computed once the exact pressure distribution is known. However, this distribution is a result of inviscid–viscous interaction of the separation bubble with the mean flow, for example, the well-known characteristic pressure plateau in a LSB is a result of this effect, which implies the necessity of including the whole separation bubble inside the domain to obtain the true pressure distribution.

With detailed measurements available, it might be possible that the measured velocity distribution (Fig. 1b) at the upper domain boundary would be usable for a calculation leading to a steady state with reverse flow at the outflow boundary, instead of the time-averaging procedure used here. However, we believe that this reverse flow would pose a serious problem for specification of outflow boundary conditions. In the present ansatz, this problem is avoided because boundary conditions are only necessary for disturbance quantities, which can simply be ramped down to zero using the already mentioned buffer-domain technique.

Test Cases B

Several combinations of disturbance excitation constitute the test cases of this section. Disturbance amplitudes for the wall-normal velocity are given in Table 2. In the experiment, mode (0, 2) is the largest disturbance observable in the first part of the LSB (Fig. 7); thus, all cases B were especially designed to study the behavior of this mode.

The inflow boundary is positioned upstream of the displacement body, $x_L = -400$ mm), before strong acceleration sets in (Fig. 1b). The outflow boundary was located at $x = 296$ mm. The wall-normal

Table 2 Disturbance v-amplitudes for cases B

Case	(0, 1)	(0, 2)	(1, 0)	(1, 1)	(1, 2)
B^{01}	0.0118	——	——	——	——
B_{01}	0.0040	——	——	——	——
B^{02}	——	0.026	——	——	——
B_{02}	——	0.0029	——	——	——
B^{11}	——	——	——	0.02	——
B_{11}	——	——	——	0.0067	——
B_{10-12}	——	——	0.010	——	0.010

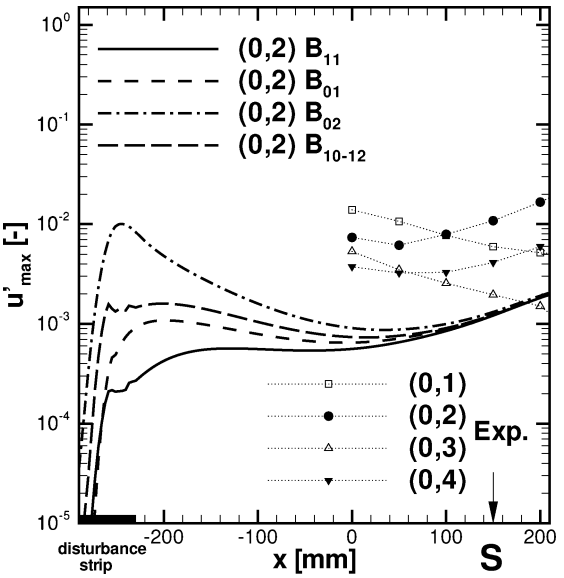

Fig. 7 Amplification of the max. steady spanwise-harmonic velocity $u'_{\max}(0, k)$, comparison of all cases B_{xx}: lines, DNS and symbols, LDA.

extent of the integration domain was raised to $y_L = 80$ mm. Its spanwise extent again is a single-spacer wavelength. The numbers of grid-points n and modes k were $n_x \times n_y \times k_z = 1538 \times 241 \times 6$, with 128 grid points in x and 10 grid points in y used for a buffer zone at the outflow and upper boundary, respectively. Discretization in x results in approximately 128 grid points per streamwise wavelength of the fundamental wave. Such a streamwise resolution was necessary during the full transition simulations to obtain the proper time-averaged flowfield and then left unchanged subsequently for simplicity.

Low resolution in the spanwise direction is justified because no breakdown into turbulence occurs in the calculations of this section. Therefore, except for the initial generation of disturbance modes by nonlinear interaction, no further mutual influence of modes took place downstream. Discretization in the wall-normal direction was found to be crucial in some cases. Thus, grid points were clustered at the wall according to the following formula ($1 \le j \le n_y$):

$$y_j = y_L\left\{(1-\kappa)\cdot[(j-1)/(n_y-1)]^3 + \kappa\cdot[(j-1)/(n_y-1)]\right\}$$

In the presented calculations, κ was chosen to be 0.1562, which resulted in an approximately 5.2 times shorter wall distance of the wall next grid point compared to an equidistant spacing. Resolution in time was raised to 900 time steps per fundamental period, necessary for the present explicit time integration due to small wall-normal grid spacing. Calculating up to the 20th period of the fundamental frequency proved to be sufficient to obtain converged results for the steady disturbances. This was checked by a calculation up to the 120th period, which did not visibly differ from the presented results and which showed a difference between results from one period to the next of $\approx 10^{-8}$ for the steady perturbations. To lower the difference by one order of magnitude took approximately 50 periods, which means that at the 20th period, results from one period to the next showed a difference of $\approx 10^{-6}$. The disturbance strip was 128 grid points in length and centered at $n_x = 320$.

Results

A comparison of disturbance amplitude development for all four cases reveals that the initial behavior of the maximum streamwise velocity perturbation differs considerably from case to case (Fig. 7). Except for case B_{11}, all calculations predict damping of the disturbance at first. After a long transient downstream development, differences in amplification rates become less pronounced until the same disturbance development is reached from $x \approx 150$ mm onward. In addition, this final state shows the same amplification rate as in the experiment.

An explanation for the initially different behavior can be derived from looking at the wall-normal amplitude distributions. These are shown for two cases in Fig. 8 for all three velocity components at two streamwise positions, $x = -100$ and 200 mm. At the first position, both cases show considerably different amplitude functions for the wall-normal velocity v and the spanwise velocity w. In case B_{11}, a streamwise vortex is developed, which can be seen from the fact that w changes its sign, whereas v keeps the same sign for all y. In contrast, the perturbation in case B_{02} is merely a streak. Despite strong differences in v and w, it is remarkable how similar amplitude functions for u look in both cases.

In Fig. 9, the same amplitude distributions for case B_{11} are compared with experimental results, as far as these are available. Fair agreement at the upstream position shows that it is very likely that steady perturbations observed in the experiment are indeed a result of nonlinear generation caused by a fluctuating disturbance, for example, (1, 1). This hypothesis will further be justified later. At the second x position, which is already inside the separation region, agreement is almost perfect, even for the very small v amplitude.

A remarkable feature of the disturbances is that, in contrast to TS-like perturbations, which show the same order of magnitude for both u and v (and exactly the same amplitude toward the edge of the boundary layer), v and w amplitudes of the steady disturbance are considerably lower than the u amplitude (more than one order of magnitude. (Note the different axis scalings in Figs. 8 and 9.)

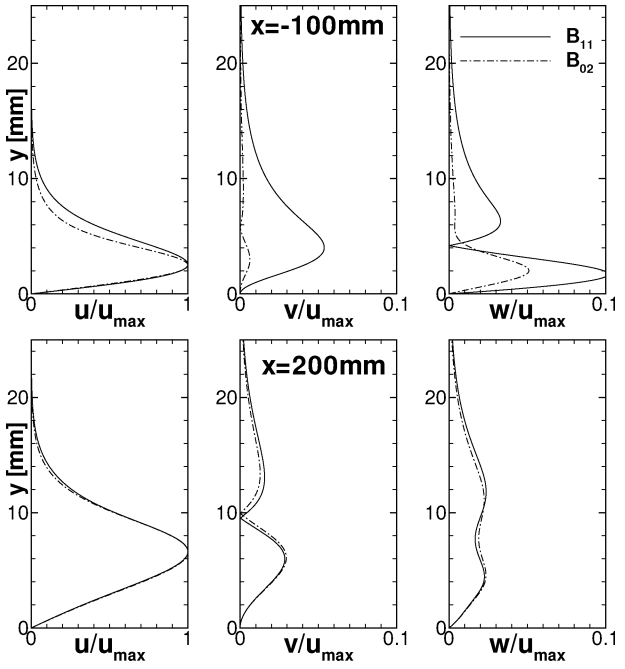

Fig. 8 Velocity amplitudes of mode (0, 2), normalized by their respective u'_{max}; comparison of case B_{11} and B_{02}.

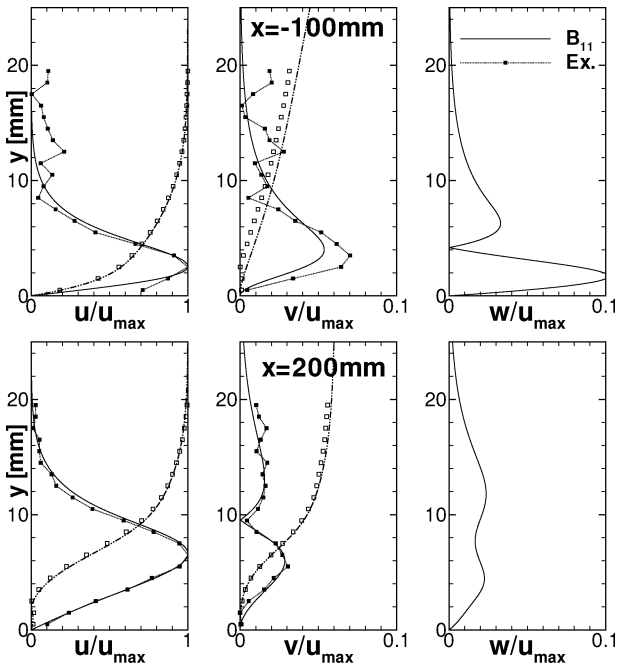

Fig. 9 Same as Fig. 8; comparison of case B_{11} with measurements, as far as available as well as mean flow quantities (0, 0).

Because the same relation can be seen for base flow quantities u and v, it appears appropriate to introduce a boundary-layer scaling for v and w. This is in line with analysis of Görtler flows (see Ref. 20).

To confirm the earlier hypothesis about the origin of mode (0, 2), simulations B^{01} and B^{02} with higher disturbance amplitudes are carried out. As can be seen in Fig. 10, perfect agreement with the experiment for mode (0, 2) is observed now in case B^{01}. However, this calculation predicts too high an amplitude for mode (0, 1).

In contrast, it was not possible to disturb mode (0, 2) directly with a high enough amplitude for the experimentally observed disturbance level to be reached because nonlinear effects appeared to set in, which resulted in a different behavior of that perturbation (not shown). However, even on the slightly too low level in case

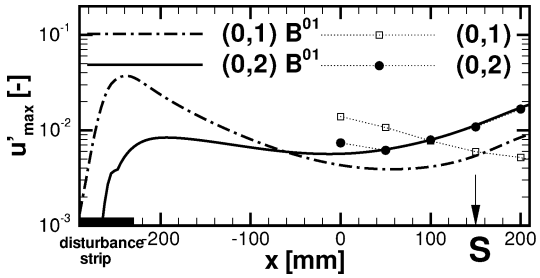

Fig. 10 Same as Fig. 7; comparison of case B^{01} with measurements.

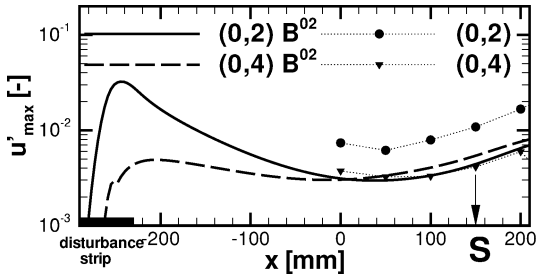

Fig. 11 Same as Fig. 7; comparison of case B^{02} with measurements.

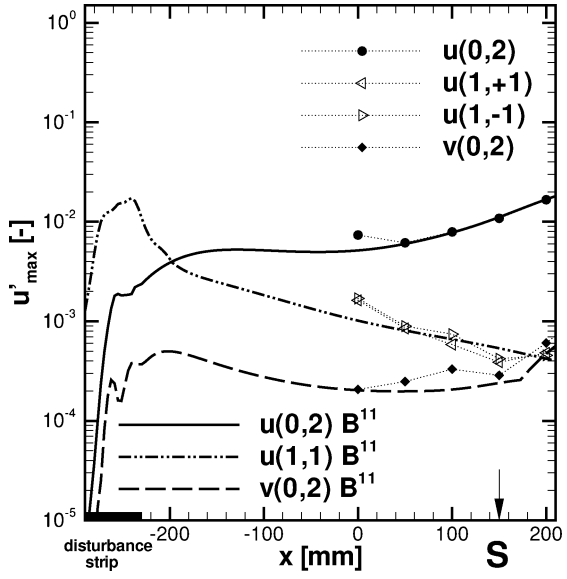

Fig. 12 Comparison of case B^{11} with measurements for streamwise and wall-normal velocities.

B^{02} as shown in Fig. 11, a far too large mode (0, 4) is developed. Thus, both cases are unable to model the situation observed experimentally. Interaction of modes (1, 0) and (1, 2) (case B_{10-12}) would also be appropriate but gives slightly less favorable comparison to the experiment than case B_{11} at upstream x positions. In addition, a higher amplitude of both generating modes would be necessary.

Finally, a simulation with adapted amplitude of mode (1, 1) was run (case B^{11}). Results are compared against measurements in Fig. 12. Note that not only predicted growth rate and amplitude of mode (0, 2) compare favorably with experimental results, but also amplitude level and decay rate of the disturbed mode (1, 1) match quite well.

Discussion

Four distinct methods for disturbance input of a steady spanwise harmonic showed different initial behavior, but developed downstream toward the same state. No difference was seen in final shape and growth rate of the disturbance, whether it arose out of a vortex or out of a streak. The development of the steady disturbance inside the separation bubble can, therefore, be considered to be independent of initial condition, however, only after a long transient region of disturbance development. This indicates that a preferred state for example, in the sense of the least damped or modal state, is reached inside the LSB, as it would if a Görtler instability existed. However, as can be seen from the amplitude function inside the bubble, the present state is not a vortex as predicted for a Blasius boundary layer on a curved surface (see Ref. 20). For that reason, the present instability will be denoted only Görtler-like.

From the favorable comparison of numerical results with measurements, it can be concluded that the steady disturbance (0, 2) is indeed a spanwise-harmonic wave and not part of a localized structure, justifying the Fourier ansatz and the low spanwise resolution in the DNS. Furthermore, this indicates that despite its fairly large amplitude of up to $\approx$3% of the freestream velocity, growth of mode (0, 2) can still be considered to be linear. A comparison of cases B_{11} and B^{11} further supports this hypothesis by showing the same development independent of amplitude. This is in line with observations of Görtler vortices in Blasius flow, which nonlinearly saturate only at an amplitude of 10% (see Ref. 20).

In an LSB, the wall-normal velocity is responsible for streamline curvature, and thus, such streamline curvature caused by boundary-layer separation is inherently a nonparallel effect. Because classical Görtler theory (see Saric[23]) neglects the wall-normal velocity and it is the curvature that causes disturbance amplification, such a theory appears not to be applicable. In contrast, for LST based on the Orr–Sommerfeld equation, strong amplification of traveling waves is a result of an inflection point in the streamwise velocity profile, which also causes a strong wall-normal velocity component but not vice versa. Thus, such a theory is more likely to be applicable, confirmed by good agreement of theoretical predictions with DNS.[14]

One possible explanation for the fact that steady disturbances need a much higher amplitude for saturation to occur when compared to traveling waves, for example, TS waves, might be given by the large difference between maximum amplitudes of u on the one hand and v and w on the other hand. It has already been stated that, for a TS wave, u and v are of the same order of magnitude (visible through joint exponential decay in y direction at the edge of the boundary layer, e.g., Fig. 6 in Ref. 14), whereas for the streaks a boundary-layer scaling [factor $\sqrt{(Re)}$] seems appropriate: The u disturbance is of the same order as the base flow u, whereas the v disturbance is of the same order as the base flow v if both are scaled by the respective $u_{\max}$. This suggests that saturation is reached whenever the v amplitude reaches high enough levels when compared to the streamwise base flow velocity, which could explain why for the steady streaks a very high u amplitude is observable even though it still shows linear behavior, whereas for a TS wave the saturation level can be considerably lower for the streamwise velocity. From this point of view, the wall-normal velocity appears to be the driving force of the physical processes.

As emphasized earlier, amplitude functions for u appear similar in all cases even at upstream x positions, whereas v and w can be considerably different. This clearly demonstrates that fairly good agreement of u-amplitude functions with experimental data is not sufficient to determine the type of disturbance and, thus, to be used for validation purposes, as it is often done in studies of transient growth. Furthermore, it stresses the need for measurements of at least two but better all three velocity components for studies of transient growth. Otherwise, such a comparison can be misleading because, as demonstrated before, a similar u-amplitude function can either lead to growth or decay, depending on initial v and w shape and amplitude (when normalized by $u_{\max}$). The streamwise distance of transient growth can be very long, here it was about 100 times the boundary-layer displacement thickness at $x = 0$ mm.

It is often argued that the stabilizing influence of a region of favorable pressure gradient can serve to damp out disturbances.[1] This is definitely true for fluctuating disturbances as can be seen from, for example, the decay of mode (1, 1) in Fig. 12. However, this is not always true for steady perturbations that might only weakly decay or even be amplified due to transient growth. This could be the reason for the occurrence of streaks observed[1] in conditions similar

to those considered here for which an explanation has not yet been found.

Conclusions

The role of three-dimensional steady disturbances and traveling waves with high-obliqueness angle was studied in detail by means of DNS. Based on a reference case, a variation of initial amplitude of steady and unsteady three-dimensional perturbations was performed to study the influence of different combinations of disturbance input.

It was shown that steady spanwise harmonic perturbations up to 3% amplitude do not influence the transition process in the LSB under consideration. Because steady perturbations typically possess growth rates that are considerably lower[11,19] than those of traveling waves in LSBs, it is very unlikely that these disturbances gain a sufficiently high amplitude, that is, $>10\%$, to dominate directly the transition process by either suppressing growth of TS waves[19] and, therefore, delaying transition, or via a secondary instability[20,21] resulting in transition enhancement. Instead, unless very strong steady three-dimensional forcing is applied, the traveling wave will always win over the steady disturbance.

A large steady three-dimensional disturbance had hardly any effect on the development of the fundamental two-dimensional TS wave. In addition, no influence was seen on transition location, which is attributed to the effect of the two-dimensional wave. This is consistent with the type of secondary absolute instability suggested by Maucher et al.,[10] which by character should not depend on initial amplitudes of the incoming three-dimensional disturbances. Strong amplification of fluctuating three-dimensional perturbations in the reference case should be attributed to nonlinear interaction merely to explain experimentally observed[12] growth rates, whereas transition is caused by the absolute instability.

Unlike the result of Wilson and Pauley,[5] steady streamwise vortices did not show up in the first part of the separated region despite spanwise harmonic forcing. However, their evidence shown was a picture of instantaneous velocity contours at a further downstream position close to the transition location, where the flow probably is already highly unsteady. The results here indicate that Görtler-like steady growing disturbances, that is, modes, might also be streaks rather than vortices and might be expected mainly in the first part of the LSB because fluctuations are far too high at the transition location to speak of curved streamlines, which is a necessary condition for a Görtler mechanism to be in operation. Furthermore, it appears that the formation of these modes can hardly be the direct route to shear layer breakdown, except in cases with extremely high initial amplitude (so-called bypass transition) as it was earlier argued to be necessary.

Our results do not contradict results of Pauley[4] that show an increased spanwise-averaged length of the separation bubble when adding spanwise sine-wave perturbations. Whereas she compared two- and three-dimensional computations, in the present study all simulations, even those without forcing three-dimensional disturbances, for example, case A_{no3D}, lead to an immediate full three-dimensional breakdown of the shear layer.

Present results support the second part of the conclusion in Ref. 11, that "simulations with forced Görtler modes may be misguided; and stationary imperfections in an experiment may not be harmful" (p. 348). In the light of our results, simulations with forced Görtler modes in an LSB are not misguided in the sense that they change the results but more in the sense that these disturbances can be strongly forced and might appear in, but are not relevant for, the transition process. When it is assumed that a similar transition mechanism is in operation in both cases, observations from this study suggest that a division into primary and secondary instability is meaningful despite the sudden breakup of the spanwise vortex into small-scale turbulence.

Acknowledgments

Financial support of this research by the Deutsche Forschungsgemeinschaft (German Research Foundation) under Grant Wa 424/19-1 and Ri 680/10-1 is gratefully acknowledged. The authors thank Matthias Lang for providing detailed experimental results used for comparison here.

References

[1]Watmuff, J., "Evolution of a Wave Packet into Vortex Loops in a Laminar Separation Bubble," *Journal of Fluid Mechanics*, Vol. 397, 1999, pp. 119–169.

[2]Rist, U., and Maucher, U., "Investigations of Time-Growing Instabilities in Laminar Separation Bubbles," *European Journal of Mechanics—B/Fluids*, Vol. 21, 2002, pp. 495–509.

[3]Inger, G., "Three-Dimensional Heat- and Mass Transfer Effects Across High-Speed Reattaching Fows," *AIAA Journal*, Vol. 15, No. 3, 1977, pp. 383–389.

[4]Pauley, L., "Response of Two-Dimensional Separation to Three-Dimensional Disturbances," *Journal of Fluids Engineering*, Vol. 116, 1994, pp. 433–438.

[5]Wilson, P., and Pauley, L., "Two- and Three-Dimensional Large-Eddy Simulations of a Transitional Separation Bubble," *Physics of Fluids*, Vol. 10, No. 11, 1998, pp. 2932–2940.

[6]Reshotko, E., "Transient Growth: A Factor in Bypass Transition," *Physics of Fluids*, Vol. 13, No. 5, 2001, pp. 1067–1075.

[7]Boiko, A. V., "Development of a Stationary Streak in a Local Separation Bubble," Inst. for Fluid Mechanics, DLR-IB 224-2002 A04, DLR, German Aerospace Center, Göttingen, Germany, 2002.

[8]Yang, Z., and Voke, P., "Large-Eddy Simulation of Boundary-Layer Separation and Transition at a Change of Surface Curvature," *Journal of Fluid Mechanics*, Vol. 439, 2001, pp. 305–333.

[9]Rist, U., "Nonlinear Effects of 2D and 3D Disturbances on Laminar Separation Bubbles," *Proceedings of IUTAM Symposium on Nonlinear Instability of Nonparallel Flows*, edited by S. Lin, Springer, New York, 1994, pp. 324–333.

[10]Maucher, U., Rist, U., and Wagner, S., "Secondary Instabilities in a Laminar Separation Bubble," *Notes on Numerical Fluid Mechanics*, edited by H. Körner and R. Hilbig, Vol. 60, Vieweg Verlag, Wiesbaden, Germany, 1997, pp. 229–236.

[11]Spalart, P., and Strelets, M., "Mechanisms of Transition and Heat Transfer in a Separation Bubble," *Journal of Fluid Mechanics*, Vol. 403, 2000, pp. 329–349.

[12]Lang, M., Marxen, O., Rist, U., and Wagner, S., "Experimental and Numerical Investigations on Transition in a Laminar Separation Bubble," *New Results in Numerical and Experimental Fluid Mechanics III*, edited by S. Wagner, U. Rist, H.-J. Heinemann, and R. Hilbig, Vol. 77, Notes on Numerical Fluid Mechanics, Springer-Verlag, Heidelberg, Germany, 2002, pp. 207–214.

[13]Lang, M., Rist, U., and Wagner, S., "Investigations on Controlled Transition Development in a Laminar Separation Bubble by Means of LDA and PIV," *Experiments in Fluids*, Vol. 36, No. 1, 2004, pp. 43–52.

[14]Marxen, O., Lang, M., Rist, U., and Wagner, S., "A Combined Experimental/Numerical Study of Unsteady Phenomena in a Laminar Separation Bubble," *Flow, Turbulence, and Combustion*, Vol. 71, Kluwer Academic Publishers, 2003, pp. 133–146.

[15]Alam, M., and Sandham, N., "Direct Numerical Simulation of 'Short' Laminar Separation Bubbles with Turbulent Reattachment," *Journal of Fluid Mechanics*, Vol. 410, 2000, pp. 1–28.

[16]Maucher, U., Rist, U., and Wagner, S., "Refined Interaction Method for Direct Numerical Simulation of Transition in Separation Bubbles," *AIAA Journal*, Vol. 38, No. 8, 2000, pp. 1385–1393.

[17]Kloker, M., "A Robust High-Resolution Split-Type Compact FD Scheme for Spatial Direct Numerical Simulation of Boundary-Layer Transition," *Applied Scientific Research*, Vol. 59, 1998, pp. 353–377.

[18]Rist, U., Augustin, K., and Wagner, S., "Numerical Simulation of Laminar Separation-Bubble Control," *New Results in Numerical and Experimental Fluid Mechanics III*, edited by S. Wagner, U. Rist, H.-J. Heinemann, and R. Hilbig, Vol. 77, Notes on Numerical Fluid Mechanics, Springer-Verlag, Heidelberg, Germany, 2002, pp. 181–188.

[19]Mendonça, M., Morris, P., and Pauley, L., "Interaction Between Görtler Vortices and Two-Dimensional Tollmien–Schlichting Waves," *Physics of Fluids*, Vol. 12, No. 6, 2000, pp. 1461–1471.

[20]Lee, K., and Liu, J., "On the Growth of Mushroomlike Structures in Nonlinear Spatially Developing Goertler Vortex Flows," *Physics of Fluids A*, Vol. 4, No. 1, 1992, pp. 95–103.

[21]Andersson, P., Brandt, L., Bottaro, A., and Henningson, D., "On the Breakdown of Boundary Layer Streaks," *Journal of Fluid Mechanics*, Vol. 428, 2001, pp. 29–60.

[22]Gaster, M., "The Structure and Behaviour of Laminar Separation Bubbles," CP-4, AGARD, 1966, pp. 813–854.

[23]Saric, W., "Görtler Vortices," *Annual Review of Fluid Mechanics*, Vol. 26, 1994, pp. 379–409.

J. Gore
Associate Editor